NANO LETTERS

2007
Vol. 7, No. 5
1129−1133

Voltage-Induced Dependence of Raman-Active Modes in Single-Wall Carbon Nanotube Thin Films

Giovanni Fanchini,* Husnu Emrah Unalan, and Manish Chhowalla

Materials Science and Engineering, Rutgers University, Piscataway, New Jersey 08854

Received October 13, 2006; Revised Manuscript Received February 9, 2007

ABSTRACT

We report on electrical Raman measurements in transparent and conducting single-wall carbon nanotube (SWNT) thin films. Application of external voltage results in downshifts of the D and G modes and in reduction of their intensity. The intensities of the radial breathing modes increase with external electric field related to the application of the external voltage in metallic SWNTs, while decreasing in semiconducting SWNTs. A model explaining the phenomenon in terms of both direct and indirect (Joule heating) effects of the field is proposed. Our work rules out the elimination of large amounts of metallic SWNTs in thin film transistors using high field pulses. Our results support the existence of Kohn anomalies in the Raman-active optical branches of metallic graphitic materials.

Transparent and conducting single-wall carbon nanotube (SWNT) thin films are two-dimensional, low-density networks of SWNTs[1] which are interesting both fundamentally and technologically. Recently, it has been noticed[2] that the Drude relaxation times in SWNT thin films, and therefore their optoelectronic properties, are controlled by intertube processes. This is an important difference with respect to individual SWNTs where intratube processes dominate.[3] The intertube processes in SWNT thin films arise from the tube to tube transport because the distance between the electrodes (∼20 μm) is typically much larger than the SWNT length. The transport properties in these networks can be explained by the percolation theory.[1]

Technologically, the ability to tailor the optical absorption coefficient and conductivity of SWNT thin films over several orders of magnitude makes them attractive for transparent and flexible electronics.[4−7] During SWNT thin film transistor fabrication, it is a common practice to precondition the SWNT network using high voltage pulses to improve the on/off ratio through supposed preferential elimination of metallic SWNTs by Joule heating.[4−7] This effect is claimed on the basis of the decrease in channel conductivity and a similar effect occurring in individual SWNTs, but little information on the modifications of the SWNTs in thin films after voltage application is available and a Raman study is still lacking.

In this Letter, we report on the Raman measurements of SWNT thin films recorded under external voltages. We have found that, although the conductivity strongly decreases, the changes in the Raman peaks are to the largest extent reversible. The films were deposited on glass using the method of Wu et al.[8] from 10, 30, and 50 mL of a 2 mg/L suspension of purified HiPCO SWNTs.[2,9] Gold electrodes (width 1 mm, distances 20 and 60 μm) were defined on each substrate. External voltages of 0−15 V (leading to electric fields $E_{ext} = 0-7500$ V cm^{-1}) were applied during the Raman measurements using a GW GPS-1850D power supply. The spectra were recorded in air on a Renishaw InVia spectrometer. Our setup for electrical Raman measurements is presented in Figure 1a. Low laser powers (12.5 μW/μm^2 at 1.96 eV excitation, 25 μW/μm^2 at 1.57 eV) were used and tested to not produce laser heating. The current was simultaneously monitored using a Keithley 195A multimeter. Each series of Raman spectra at the varying voltage was recorded on the same spot in order to attain comparable signal intensity. After any measurment at a given external field, sufficiently low field (500 V/cm, leading to undetectable changes in the Raman signal) was applied so that a low-field Raman spectrum and the sample conductance could be recorded.

The typical variation of the G-bands[3] and the doubly resonant D-band[10] under the influence of an electric field are shown in parts b and c of Figure 1, respectively. A clear decrease in peak position (Ω) and intensity (I_S) for both bands with increasing electric field (E_{ext}) can be observed. Similar shifts in the Raman bands under the influence of electric fields have been observed in ferroelectrics.[11] In contrast, electrochemical Raman measurements of SWNT electrodes in aqueous environments[12] resulted in upshifts of the G-bands, which clearly points to differences between our and such experiments. Electromechanical Raman measurements may lead to both upshifts or downshifts.[13]

10.1021/nl062418m CCC: $37.00
Published on Web 03/30/2007

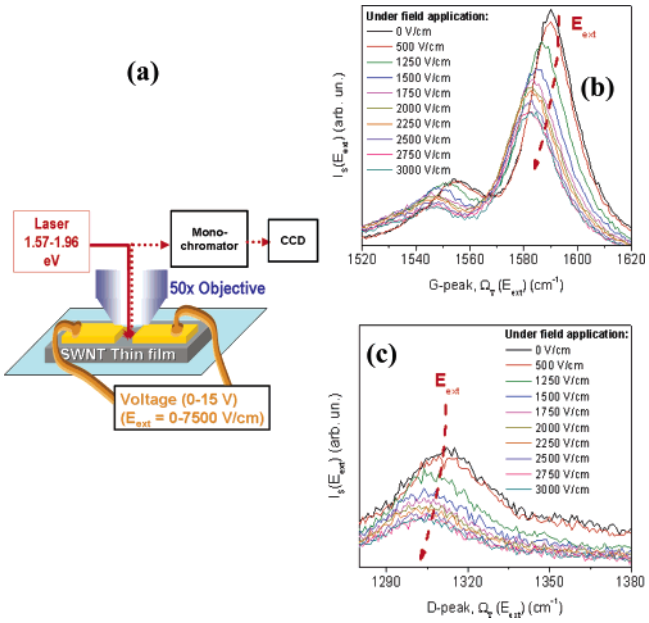

Figure 1. (a) Schematic of the setup for electrical Raman measurements. Typical dependence of the Raman modes on the electric field (E_{ext}) (b) for the G peak (excitation energy $\hbar\omega = 1.96$ eV) and (c) for the D peak. From panels b and c, the two main effects, peak downshifts and decrease in peak intensities, are evident.

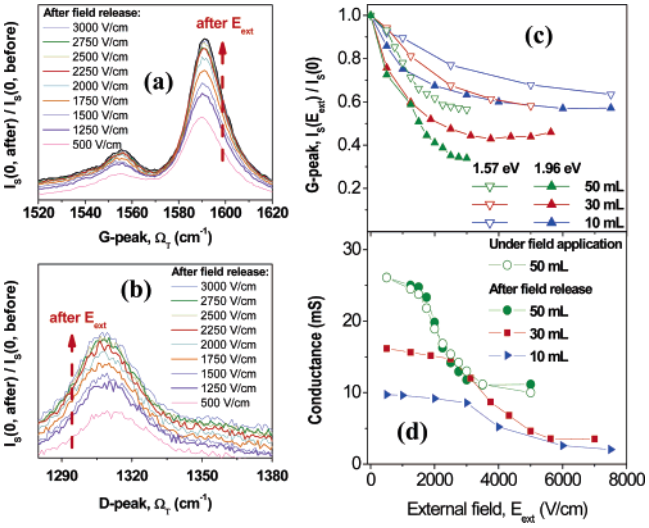

Figure 2. Permanent increase of the low-field intensities of (a) the G peak and (b) the D peak. Data in panels a and b are recorded at the same runs as panels b and c of Figure 1. (c) Dependence of the Raman G-peak intensities on the electric field (E_{ext}). (d) Permanent decrease in sample conductance is measured, and it does not recover after the electric field is released.

Parts a and b of Figure 2 show the Raman peaks recorded immediately after releasing each external field used for the measurements shown in parts b and c of Figure 1. The recovery of the G and D peaks to their original frequencies is evident. Peak intensities not only recover but also increase slightly compared to their pristine value before field application. From the data in Figure 2a,b we conclude that the observed effects on the G and D peaks are indeed reversible. The data from Figures 1b and 2a are summarized in Figure 2c, showing the ratios between the intensity of the G-bands

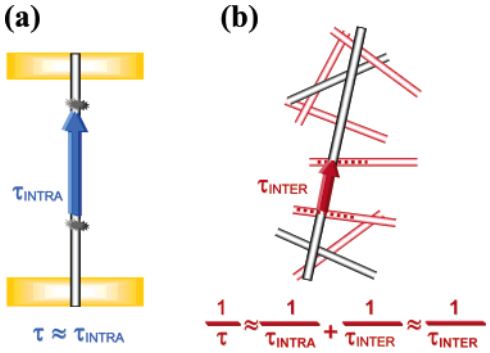

Figure 3. Schematics of (a) intratube processes (mostly related to electron−phonon interaction) and (b) intertube processes (related to cross links of different SWNTs) in determining relaxation times. Intratube processes control the performance of individual SWNTs. Intertube processes prevail in SWNT films where each m-SWNT (depicted in black) is cross linked by many other nanotubes, including semiconducting ones (depicted in red).

before and after the external field release for the samples and excitation energies investigated in this study.

While the Raman effects in our experiments are reversible, the conductance does not recover after the external field release (Figure 2d). Similar decrease in conductance has been found to improve the on/off ratio of thin film transistors and claimed to be due to burning of metallic SWNTs.[4−7] In our study, the reversibility in decrease of the peak intensities rules out the burning of large amounts of SWNTs. We corroborate this by analyzing the radial breathing mode (RBM) of (n,m)-SWNTs in our films, as discussed below.

It is tempting to assign the observed downshifts to voltage-induced Joule heating, increasing the temperature of the films. Although alternative hypotheses can be easily dismissed,[14] it is crucial to clarify the origin and the amount of Joule heating itself, which must be expectedly large in order to justify the observed behavior. It was calculated[15] that strong selective heating of Raman-active phonon modes (up to $T \sim 10^4$ K in *individual* metallic SWNTs) occurs in the presence of current due to Kohn anomalies.[16] Figure 1, however, shows that the linewidth of the G and D bands does not appreciably increase with electric field, as it would do in the presence of a strong increase in phonon temperature. Therefore, we will discuss our results in terms of moderate Joule heating in the presence of Kohn anomalies in an adiabatic system dominated by intertube interactions. This leads to strong electric-field-dependent fluctuations in the dielectric response of SWNT films, with the same mechanism leading to fluctuations of the Raman frequencies in ferroelectrics.[11]

Let us first recall that in percolating SWNT networks, the electronic confinement is released and the wave functions extend over several SWNTs, both semiconducting (s-SWNTs) and metallic (m-SWNTs), and τ, the Drude relaxation times, depend on the network density and not on intrinsic properties of SWNTs.[2] The intra- and intertube processes for an individual SWNT and a network of SWNTs are schematically shown in Figure 3a,b. In a system where both intra- and interparticle processes contribute to the transport mechanisms and the relaxation of electron mo-

menta, the effective relaxation time can be written according to Matthiessen's rule[17] as

$$\frac{1}{\tau} = \frac{1}{\tau_{\mathrm{INTRA}}} + \frac{1}{\tau_{\mathrm{INTER}}} \tag{1}$$

where τ_{INTRA} and τ_{INTER} represent the intratube and intertube relaxation times, respectively. Therefore, τ is dominated by the shorter of τ_{INTRA} or τ_{INTER} which, in SWNT thin films where each tube is interconnected to many others, is clearly the latter. Relaxation indicates that the external field displaces the Fermi sphere through a shift in momentum $\hbar\Delta k$[18]

$$\hbar\Delta k = e\cdot\tau\cdot E_{\mathrm{ext}} \tag{2}$$

where e is the electron charge.

Let us now recall that the strong Raman activity of the G and D bands of metallic SWNTs should correspond to exceptionally strong electron−phonon coupling,[3,10,19] whose origin had been unclear for a long time. Recently, Piscanec et al.[16] offered an explanation through demonstration of the existence of Kohn anomalies in the screening of ions in metallic graphitic materials. In general, Kohn anomalies occur when the size of the Fermi surface is comparable to the phonon wavevector $\mathbf{q}$.[16,20−22] As discussed by Piscanec et al.,[16] the π and π^* bands in graphite and m-SWNTs touch the Fermi level (E_F) at the **K**-point which results in a very small Fermi wavevector ($\mathbf{k_F} \sim \mathbf{0}$) whose modulus approaches those of the G and D phonon wavevectors ($\mathbf{q} = \mathbf{\Gamma} = \mathbf{0}$ and $\mathbf{q} = \mathbf{q'} - \mathbf{K} = \mathbf{0}$). Since $|2\mathbf{k_F}|^{-1}$ represents the typical scale length for screening a pointlike disturbance,[22] the condition $\mathbf{q} \sim 2\mathbf{k_F} \sim \mathbf{0}$ requires that infinite distance is needed for the electrons to fully screen an optical phonon.

It is well-known that Kohn anomalies in one-dimensional (1-D) solids lead to logarithmic divergence of the static dielectric response, $\epsilon(q\sim 2k_F, \hbar\omega\sim 0)$, while in 3-D solids the divergence only affects the first derivative of this quantity. Dealing with 1-D electronic structures, it is then obvious that small fluctuation in the electron momenta (e.g., by applying a constant external field) corresponds to strong, non-negligible, fluctuation in the dielectric response.[23] We shall treat such fluctuations in the framework of the Lindhard model.[24] Accordingly, the dynamic dielectric response of the anomalously screening electrons in the presence of a change in momentum $\hbar\Delta k(E_{\mathrm{ext}})$ is given by[22]

$$\epsilon[\Delta k(E_{\mathrm{ext}}),\hbar\omega] - 1 = -4e^2\epsilon_0 \lim_{\substack{k_F\to 0 \\ q/2k_F\to 1}} \int \mathrm{d}k \frac{f(k_F + \Delta k + q/2,T) - f(k_F + \Delta k - q/2,T)}{\in_{k+\Delta k+q/2} - \in_{k+\Delta k-q/2} - \hbar\omega} \tag{3}$$

where ϵ_0 is the dielectric response in vacuum and the Fermi−Dirac population probability $f(k,T)$ will be taken to be approximately linear in the energy domain $E_F \pm k_BT/2$ and 1 or 0 elsewhere. Since the dielectric responses obtained from ellipsometry at our Raman excitation energies ($\hbar\omega = 1.57-1.92$ eV) follow a Drude behavior,[2] $\in_k$ will be taken to be the dispersion relation for free electrons ($\in_k = \hbar^2k^2/2m$). Similar conclusions however can be also anticipated when assuming a linear band structure for $\in_k$ as customary for individual SWNTs. Care should be taken in evaluating eq 3, because very slight changes in q, ω, and T can lead to fluctuations of $\epsilon(q,\hbar\omega)$ from 1 to infinity.[23] Therefore, since a very small value of k_F is expected in our percolating networks, we estimate eq 3 at k_F tending to zero with the same zeroth order of q, thus leading to a finite ratio $q/2k_F \to 1$. Evaluation of eq 3 gives $\epsilon(0, \hbar\omega>0) - 1 = 0$ in the absence of electric field, while in the presence of field

$$\epsilon(\Delta k,\hbar\omega) - 1 = \frac{8e^2}{\epsilon_0 k_B T}\left(\sqrt{\frac{mk_BT}{\hbar^2} + \Delta k^2} - \sqrt{\frac{mk_BT}{\hbar^2} - \Delta k^2}\right) \tag{4}$$

for

$$k_BT \gg \frac{\hbar^2\Delta k^2}{m}$$

The intensity and the frequency of the Raman-active optical phonons are related, via the electron−phonon coupling, to the dynamic dielectric response $\epsilon(q \sim 2k_F, \hbar\omega)$.[22] Therefore, knowledge of the dynamic dielectric response will now allow us to extract information about the G and D mode frequencies. Especially, if the screening is assumed to (perturbed by temperature and electric field) largely determine frequencies of the screened optical phonons, then the Raman shifts in the presence [$\Omega(E_{\mathrm{ext}})$] and absence [$\Omega(0)$] of field can be related by[11,25]

$$\Omega_T(E_{\mathrm{ext}})^2\cdot\epsilon[\Delta k(E_{\mathrm{ext}}),\hbar\omega] = \Omega_T(0)^2\cdot\epsilon(0,\hbar\omega) \tag{5}$$

The anharmonic modifications of the SWNT structure can be included by assuming a temperature-dependent zero-field Raman shift $\Omega_T(0) \approx \Omega_{300K}(0) - X_TT$ ($X_T \approx 0.01$ cm^{-1} K^{-1}, for the G peak[26]). However, we anticipate that they would not significantly affect the parameters achievable by fitting our model with the experiment (relaxation times and temperatures change below 30−40%). Replacement of $\epsilon[\Delta k(E_{\mathrm{ext}}),\hbar\omega]$ and $\epsilon(0,\hbar\omega)$ from eqs 3 and 4 into eq 5 leads to the following relation for the frequency of the Raman optical modes upon temperature and external field increase, as plotted in Figure 4a

$$\Omega_T(E_{\mathrm{ext}}) = \Omega_T(0)\left[1 + \frac{8e^2}{\hbar\epsilon_0 k_B T}\left(\sqrt{mk_BT + \frac{e^2\tau^2}{2}E_{\mathrm{ext}}{}^2} - \sqrt{mk_BT - \frac{e^2\tau^2}{2}E_{\mathrm{ext}}{}^2}\right)\right]^{-1/2} \tag{6}$$

A comparison between our model and experimental results is shown in Figure 4b,c. Fits were obtained assuming the temperature of the Raman-active phonons rising linearly from

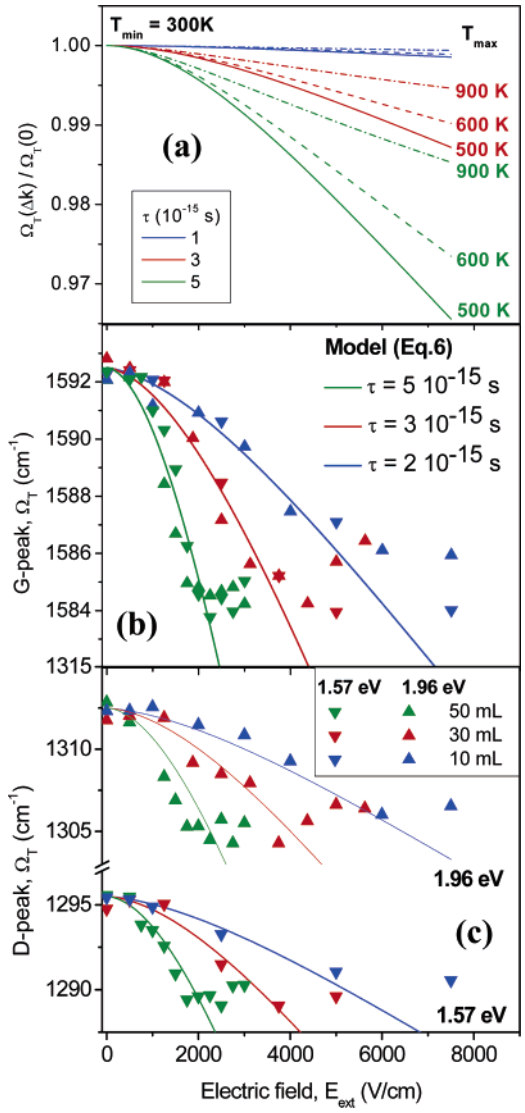

Figure 4. (a) Dependence of the Raman shifts on the electric field (E_{ext}) according to eq 6, assuming that the samples, initially at room temperature (T_{min}), heat proportionally with electric field (E_{ext}). Comparison with measured (b) G-peak and (c) D-peak frequencies. The lines represent data fits from eq 6 with $T_{max} = 600$ K and τ as reported in the legend.

$T_{min} = 300$ K to $T_{max} = 500-700$ K at external fields $E_{ext} = 0-7500$ V/cm.[27] Note that these temperatures are far too low to burn the m-SWNTs. Furthermore, strong temperature increase would have been accompanied by broadening of the G, D, and RBM peaks,[26] which we did not observe. Thus Joule heating in our films must be moderate, in agreement with the relatively low maximum temperatures (T_{max}) predicted by our model. In the framework of our model, the decrease in intensity of the Raman modes can be easily explained since the Stokes/anti-Stokes Raman cross sections $I_{S/AS} \sim |\partial\epsilon/\partial u_{||}|^2 + |\partial\epsilon/\partial u_{\perp}|^2$ [28] decrease at increasing fields in direction longitudinal to the field, while remaining unchanged in transversal directions.[29,30] Furthermore our fits lead to relaxation times of $\tau \sim (1-5) \times 10^{-15}$ s, which agree well with the ones achievable by ellipsometry.[2] Such values are of the same order of magnitude to the inverse of the G-band pulsation ($t_G \approx 3 \times 10^{-15}$ s). This is in contrast to

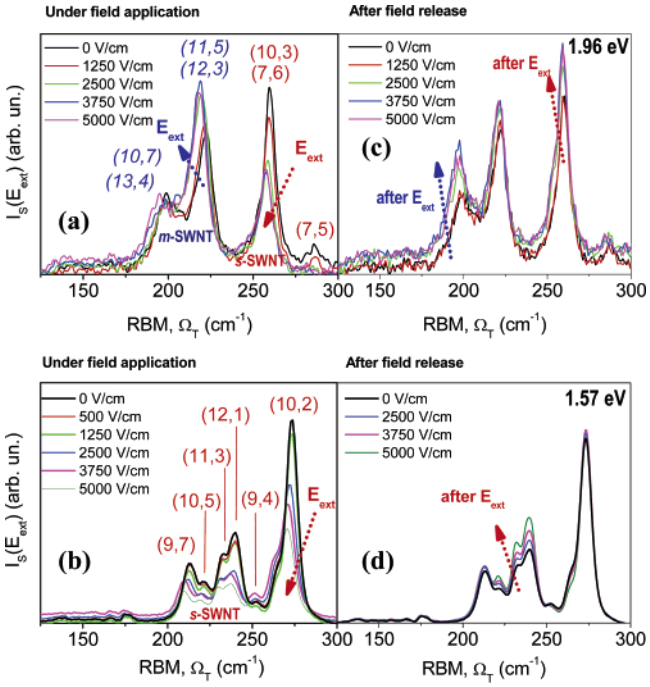

Figure 5. Modifications of the RBMs by external field at (a) 1.96 eV (exciting both m- and s-SWNTs) and (b) 1.57 eV (exciting only s-SWNTs). Assignments of specific (*n*,*m*)-SWNTs are taken from Telg et al.[32] The *reversible* decrease for s-SWNTs (red) and the *reversible* increase for m-SWNTs (blue) are shown. In contrast, after field release, the *permanent* effects are always in increasing the RBM intensities for both s- and m-SWNTs at (c) 1.96 eV and (d) 1.57 eV.

what happens in a single graphene layer[20] (or, likely, a single individual m-SWNT) where the relaxation times, being dominated by intralayer (or intratube) processes, are much longer and $t_G \ll \tau \approx \tau_{INTRA} \approx 100 \times 10^{-15}$ s,[31] leading to the breakdown of the adiabatic Born−Oppenheimer approximation. In contrast, the condition $t_G \sim \tau \approx \tau_{INTER} \sim 10^{-15}$ s, which still persists in our thin films, leads to a scenario that is still adiabatic and, thus, entirely different from the nonadiabatic behavior of the Raman spectra in the presence of Kohn anomalies as discussed in ref 20.

We have also examined the RBMs of our thin films in order to investigate the influence of the electric field on (*n*,*m*)-SWNTs with various chiralities. The RBMs are shown in parts a and b of Figure 5. It can be seen from Figure 5a that at $\hbar\omega = 1.96$ eV, where both s- and m-SWNTs are excited, the intensities of the RBMs of s-SWNTs decrease with increasing electric field while the intensities of the RBMs of m-SWNTs increase. In Figure 5b ($\hbar\omega = 1.57$ eV) where only s-SWNTs are sampled, the intensities of the RBMs decrease with increasing electric field. In contrast, after the electric field has been released, it can be seen in Figure 5c,d that the RBM intensity always slightly increases in both s- and m-SWNTs. The most interesting feature of this slight increase is that it remains permanent subsequent to the field release. Thus, the decrease in measured conductance shown in Figure 2d cannot be correlated to the claimed preferential elimination of m-SWNTs.

The increase in intensities of the RBMs of m-SWNTs is an expected effect if the increase in Boson number of the

optical phonons is the determining factor of peak intensity. The decrease in the intensities of RBMs in s-SWNTs is not consistent with Joule heating as the determining factor in controlling the intensity of the RBMs. Indeed, it can be demonstrated[14] that the decrease in RBM intensities cannot be accounted for by assuming that all the m-SWNTs are moving closer to resonance, while all the s-SWNTs are moving off resonance. Upon a temperature increase, the resonant energies[32] of some of our (n,m)-SWNTs are expected to be closer to the Raman excitation energies, 1.57 and 1.96 eV, while other (n,m) tubes will be farther from their resonant energies.[14] However this would happen without any systematic dependency on the metallic or semiconducting nature of each (n,m)-SWNT.[14] Rather, we suspect that the intensity decrease of the RBMs of s-SWNTs at increasing voltage are more likely to be related to the same causes determining the decrease of the D- and G-peak intensities.

In conclusion, we reported on the changes in Raman peaks of SWNT thin films as a function of an external electric field. We assign such effects to anomalous electron−phonon interactions. We dismiss the idea that, in SWNT thin films, voltage pulses produce Joule heating high enough to burn large amounts of m-SWNTs. This does not happen because the maximum temperatures reached in SWNT thin film devices under voltage application are much lower than in individual SWNT devices, and the relaxation times are much shorter. Rather, thermal oxidation,[33] selective cutting of the m-SWNTs, or elimination of very small amounts of m-SWNTs on some critical percolating pathways may reduce the "off" currents and improve the transistor performance. Finally, electrical Raman spectroscopy will be a new and powerful technique for characterizing thin films and devices incorporating one-dimensional nanostructures.

Supporting Information Available: Discussions of the difficulties of interpreting experiments in terms of electromechanical strain and the origin of the voltage dependency of the RBM intensities. This material is available free of charge via the Internet at http://pubs.acs.org.

References

(1) Hu, L.; et al. *Nano Lett.* **2004**, *4*, 2513.
(2) Fanchini, G.; et al. *Appl. Phys. Lett.* **2006**, *89*, 191919.
(3) Dresselhaus, M. D.; Eklund, P. C. *Adv. Phys.* **2000**, *49*, 705.
(4) Snow, E. S.; et al. *Appl. Phys. Lett.* **2003**, *82*, 2145.
(5) Zhou, Y.; et al. *Nano Lett.* **2004**, *4*, 2031.
(6) Seidel, R.; et al. *Nano Lett.* **2004**, *4*, 831.
(7) Takenobu, T.; et al. *Appl. Phys. Lett.* **2006**, *88*, 033511.
(8) Wu, Z.; et al. *Science* **2004**, *305*, 1273.
(9) Unalan, H. E.; et al. *Nano Lett.* **2006**, *6*, 2513.
(10) Thomsen, H.; Reich, S. *Phys. Rev. Lett.* **2000**, *85*, 5214.
(11) Worlock, J. M.; Fleury, P. A. *Phys. Rev. Lett.* **1967**, *19*, 1176.
(12) Corio, P.; et al. *Chem. Phys. Lett.* **2003**, *370*, 675; **2004**, *392* 396. Okazaki, K.; et al. *Phys. Rev. B* **2003**, *68*, 035434.
(13) Hartman, A. Z.; et al. *Phys. Rev. Lett.* **2004**, *92*, 236804.
(14) See Supporting Information.
(15) Lazzeri, M.; et al. *Phys. Rev. Lett.* **2005**, *95*, 236802.
(16) Piscanec, S.; et al. *Phys. Rev. Lett.* **2004**, *93*, 185503.
(17) Ashcroft, N. W.; Mermin, N. D. *Solid State Physics*; Saunders: Philadelphia, 1976; p 323.
(18) Dressel, M.; Gruner, G. *Electrodynamics of Solids*; Cambridge University Press: Cambridge, 2002.
(19) Ferrari, A. C.; Robertson, *Phys. Rev. B* **2000**, *61*, 14095.
(20) Pisana, S.; et al. *Nat. Mat.* **2007**, *6*, 198. See arXiv:cond-mat/0611714.
(21) Popov, V. N.; Lambin, P. *Phys. Rev. B* **2006**, *73*, 085507.
(22) Ashcroft, N. W.; Mermin, N. D. *Solid State Physics*; ref 17, 1976; p 515.
(23) For instance, at $T = 0$ K, eq 3 would lead to $\epsilon(\Delta k, \hbar\omega) - 1 \sim \log\{[(x + 1)^2 - (x_E + y)^2]/[(x - 1)^2 - (x_E + y)^2]\}$, with $x = q/2k_F$, $x_E = \Delta k(E_{ext})/2k_F$, and $y = m\omega/\eta q$ so that Kohn anomalies ($x = 1$) correspond, in the absence of field, to an infinite static response $\epsilon(0,0) - 1 \rightarrow \infty$ and a null dynamic response $\epsilon(0, \hbar\omega) - 1 = 0$ while, in the presence of field, $\epsilon(\Delta k, 0) - 1 \rightarrow \infty$.
(24) Actually, the use of the Lindhard model relies on the adiabatic Born−Oppenheimer approximation which, as verified below, still holds in our SWNT thin films. In contrast, our adiabatic model will be inadequate in nonadiabatic systems (e.g., graphene).
(25) Ashcroft, N. W.; Mermin, N. D. Reference 22, pp 513−523.
(26) Uchida, T.; et al. *Chem. Phys. Lett.* **2004**, *400*, 341. Zhou, Z.; et al. *J. Phys. Chem. B* **2006**, *110*, 1206. Nevertheless, while the changes achieved including possible anharmonic effects in our model are low, the influence on the electron screening of the alternating electric fields used for Raman excitation might also be considerable. This would suggest that our model might also be useful in explaining the temperature dependence of the Raman peaks of SWNT thin films in the absence of a constant external field.
(27) The relaxation times determined within our model are of the order of magnitude available in literature (see ref 22, p 10). Furthermore, straightforward Drude analysis of the ellipsometry spectra of our samples (ref 2) also leads to $\tau \sim 10^{-15}$ s. We suspect that especially intertube processes between one m-SWNT and one s-SWNT are important in lowering the relaxation times, since s-SWNTs may act as thermal sink (ref 15). Thus, the higher the participation of s-SWNTs to electrical transport, the smaller τ_{INTER}. Impurities might also contribute in decreasing both intra- and intertube relaxation times.
(28) $u_{||}$ and $u_{\perp}$ represent, in each SWNT, the modes polarization longitudinal and transversal to the electric field.
(29) Barker, A. S.; Loudon, R. *Rev. Mod. Phys.* **1972**, *44*, 18.
(30) Fanchini, G.; et al. *J. Appl. Phys.* **2002**, *91*, 1155.
(31) Zhang, Y.; et al. *Phys. Rev. Lett.* **2006**, *96*, 136806.
(32) Telg, H.; et al. *Phys. Rev. Lett.* **2004**, *93*, 177401.
(33) Jhi, S-H.; et al. *Phys. Rev. Lett.* **2000**, *85*, 1710.

NL062418M